Ocean color as a proxy to predict sea surface salinity in the Banda Sea

Ocean color as a proxy to predict sea surface salinity in the Banda Sea

Sam Wouthuyzen[1,6], E. Kusmanto[1], M. Fadli [2,6], G. Harsono[3,4], G. Salamena[2,5,6], J. Lekalette [2,6] and A. Syahailatua [1,6]

[1] Research Center for Oceanography – LIPI, Jakarta; Jl. Pasir Putih 1, Ancol Timur Timur, Jakarta 14430, Indonesia,
[2] Research Center for Deep Sea – LIPI, Ambon.
[3] Centre for Hydrography and Oceanography – Indonesian Navy, Jakarta, Indonesia,
[4] Department of Remote Sensing Technology, Indonesian Defense University, Bogor, Indonesia
[5] Graduate Research School, College of Science and Engineering, James Cook University, Australia
[6] Centre of Excellence for Tuna Conservation – Ambon, Indonesia

corresponding author: swouthuyzen@yahoo.com

Abstract. Salinity is an important ocean parameter that greatly influences physical, chemical, and biological ocean properties and processes. Salinity combines with sea temperature and chlorophyll-a (Chl-a) that mostly sourced from remote sensing-based measurements can reveal ocean quality and supports fisheries. However, the satellite-derived Sea Surface Salinity (SSS) dataset (~ 9 years) is not as temporally adequate as SST and Chl-a datasets (~3 decades) and thus, preventing a comprehensively spatio-temporal analysis of this water quality aspect. Since (SSS) can be approximated using satellite-derived ocean color products having the similar temporal length of datasets to the available SST and Chl-a datasets, predicted SSS can be produced from these ocean color products to fill the gap of the existing SSS dataset. This study aims to estimate the SSS from ocean color products of Aqua-MODIS satellite with a spatial and temporal resolution of 4 km and 8-daily by developing an empirical model. The ocean color data used were remote sensing reflectance (Rrs) of blue, green and red wavelengths (412, 433, 469, 488, 531, 547, 555, 645, 667 and 678 nm). The absorption coefficients due to detritus material non-algae, Gelbstof and CDOM (ADG) at 443 nm and the absorption coefficient due to phytoplankton (APH) at 443 nm data were also used. The Banda Sea was chosen due to its large-scale upwelling system (~300 km x 300 km) that providing an important ocean process related to fishery and the availability of in-situ salinity measurements (i.e. CTD casts from series of Research Vessel (R/V) Baruna Jaya III, VII and VIII cruises and Argo floats), which a part of these datasets will be used to validate predicted SSS. Results showed that of all ocean color parameters tested, ADG at 443 nm was strongly correlated with in-situ SSS through the polynomial order 5 regression equation with a high R^2 of 0.94 and a low RMES value of 0.101 PSU. Although this empirical model has high accuracy, but based on RMSE analysis results from various locations within and outside the Banda Sea that influenced by the Pacific and the Indian ocean water masses indicates that this model actually good to predict in-situ SSS only for a narrow range SSS of 33.4-34.5 PSU. Nevertheless, this model has a limitation, it is still can be used for predicting and mapping the SSS for Banda Sea as well as for most of the Indonesian waters. The long-term meteorological SSS map (2003-2017) derived by this model together with the SST and Chl-a maps can show clearly the upwelling phenomena of the Banda Sea, which occurred during the southeast monsoon (June-July-August, JJA). This study proves that ocean color data from Aqua-MODIS satellite can be applied to estimate and to map the SSS for most of the Indonesian waters, but validations for this model is still needed

Keywords: Ocean color, MODIS, Rrs, ADG at 443 nm, SSS, Banda Sea,

1. Introduction

Salinity is one of the important parameters in the ocean that is the most often measured in every single ocean research activity. Salinity affects many physical, chemical, and biological properties of the ocean, so that it can affect the ocean processes [1]. For example, the ocean currents/circulation that move from one place to another were influenced by the changes of horizontal pressure gradients that generated by the differences of the density of seawater, salt concentration, sea temperature and pressure [2, 3, 1]. Sea surface salinity (SSS) can be used as a tracer of freshwater input from rivers to coastal oceans, so it is potential to monitor the river plumes [3, 4, 5, 6]. Salinity can also cause various marine organisms such as fish larvae and juveniles to have different distributions based on their tolerance to salinity [7, 3]. Recently, sea surface salinity (SSS) has been used intensively for studying the global climate variability, the same as using conventional data of SST, such as the ENSO in the Pacific [8, 9, 10, 11, 12] and Indian Ocean Dipole (IOD) mode in the tropical Indian Ocean [13, 14]. However, although salinity plays an important role, conventional measurement of salinity (SSS) carried out by research vessels or using Argo floats are sparse and irregular, so large part of the global oceans have not been measured [2]. Furthermore, salinity measurement from space lags far behind the SST, Chlorophyll-a (Chl-a) and many other ocean parameters that have been used to study the local and global ocean phenomena effectively and efficiently for over 3 decades through remote sensing techniques [15].

The vacuum of salinity measurements from the space platform just can be realized after two satellite missions; the first is the Soil Moisture and Ocean Salinity (SMOS) satellite launched on November 2, 2009, by the European Space Agency (ESA), which carried a radiometer L-band (l.43GHz) named Microwave Image Radiometer using Aperture Synthesis (MIRAS) [2, 16, 17], while the second is the Aquarius / SAC-D satellite (Satelite de Aplicaciones Cientificas-D) launched on June 10, 2011, by a collaborative mission between the space agency of America (NASA) and Argentina (Comisión Nacional de Actividades Espaciales/CONAE), which carried combination sensors of passive (radiometer) and active (radar) that work also on L-band (https://salinity.oceansciences.org/news-more.htm?id=5; [18]. Both satellites were intended to be able to estimate the SSS of the global ocean with a precision of root-mean-square error (RSME) of 0.2 practical salinity units (PSU), so now they promote the global SSS observation by using remote sensing techniques [2, 18].

Since then, numerous scientific articles discussing various aspects of ocean research using SSS data derived from these satellites have been published in various scientific journals, including master's theses and doctoral dissertations. A total of 2,393 publications on ocean salinity consist of 1,910 and 483 articles that use the SMOS and Aquarius satellite data are currently recorded on ESA's web (http://www.esa.int/esasearch?q=publication+of+SMOS+on+ocean+salinity&start=11) and NASA Salinity's web (https://salinity.Ocean sciences.org/publications.cgi), respectively.

Although the results of error distribution of SSS retrieval for the global ocean (50ºS-50ºN) were relatively small with RMSE ranging from 0.25-0.35 PSU for SMOS and 0 ~ 0.2 PSU for Aquarius [19] as well as in the tropical ocean (20ºS-20ºN) of 0.289 and 0.228 PSU for SMOS and Aquarius, respectively [20]. and in the range of 0.10 ~ 0.59 PSU for Aquarius in 10 selected areas of the Bay of Bengal, tropical Indian Ocean [21]. However, both of SSS retrieval can only be used to study various aspects of the ocean at the global scale with a coarse resolution about 150-200 km [2, 3, 17], which cannot be applied to monitor and to understand the exchange/mixing SSS between land and marine system of the coastal zones [3]. In addition, within 200 km of land, the SMOS and Aquarius sensors may be contaminated by man-made radio frequency interferences (RFI) and also the leakage of land signals from soil moisture background, which may significantly resulting bias and affect the quality of the SSS data. Therefore, SSS data from such areas are often discarded [22, 23, 19]. This drawback made the SSS data in the coastal waters of many Indonesian's inner seas were mostly not available.

SSS mapping from space has actually been done more than 3 decades before the launch of the SMOS and Aquarius satellites by using ocean colour information through optical remote sensing data at visible wavelengths (400-700 nm). SSS does not have direct colour signals [24 , 25] such as chlorophyll-a or suspended solids, then it is impossible to generate direct relationship between SSS and data obtained from the sensor of ocean colour satellites. However, study pioneered by [26] and [27] and later on followed by [28, 29, 30, 31, 32, 3] showed that CDOM in many coastal seas and estuaries has often been observed strongly correlated with the inverse of salinity.

The CDOM or also called gelbstoff, or gelvin or yellow substances are humic and fulvate materials that predominantly originate from the land and then transported to the coastal waters through freshwater runoff. Close to the river, CDOM with high concentration causes waters to be green, yellowish-green or brownish in colour, while the salinity is very low. Inversely, away from the continental margin, the influence of the river becomes weak proportional to the decrease in CDOM concentration, but the salinity increases [33, 34, 35, 36, 28]. Furthermore, the optical properties of CDOM are characterized by strong absorption in the spectrum of ultraviolet (UV) and blue light than other visible wavelengths [31, 3]. Therefore, the inverse of high CDOM-low salinity and low CDOM-high salinity relationship and its optical characteristic can be used as a proxy to estimate SSS and then it is easily retrieved from various sensors of ocean colour satellites, such as SeaWiFS [37, 38, 28, 39, 24, 31, 40, 41, 42, 43] and MODIS [29, 3, 15, 44].

Instead of inverse CDOM-salinity relationship approach as mentioned above,[45] stated that SSS could also be estimated directly by using water-leaving reflectance from multiple MODIS wavebands, because dissolved salts and suspended substances have a major impact on the electromagnetic radiation attenuation in the visible spectrum range. Using direct algorithms approach, a number study has been assessed the SSS using various sensors in the various waters of the world, such as old work of [46] using Multi Spectral Scanner/MSS of Landsat in the San Franciso Bay Delta. Thematic Mapper/TM of Landsat in the large estuarine lake of the US Gulf of Mexico coast [47]; MODIS in the Hong Kong waters [45], in the South China Sea [48], in the Mid-Atlantic [3], in the Chesapeake Bay, USA [49], in the Bohai Sea, China [50, 44]. In the Northern Gulf of Mexico coast [17]. [5] using Geostationary Ocean Colour images (GOCI) satellite mapped SSS in the Osaka Bay, Japan.

NASA GES DISC (Goddard Earth Sciences Data and Information Services Center) has been developed a Web-based application that provides a simple and intuitive way to visualize, analyze, and access vast amounts of remote sensing data without having to download the data called “GIOVANNI” (an acronym for the “GES DISc Interactive Online Visualization ANd aNalysis Infrastructure) (https://giovanni.gsfc.nasa.gov/giovanni/). Among of huge data in GIOVANNI’s web, there are data of absorption coefficient of non-algal material due to gelbstoff, detrital material and CDOM (ADG) and due to Phytoplankton (APH) at 433 nm as well as remote sensing reflectance (Rrs) in the visible wavelength of Blue bands (412, 443, 469, and 488 nm), Green bands (531, 547 and 555 nm) and Red bands (645, 667 and 678 nm). Since CDOM was well proven correlated with SSS as mentioned above, and SSS can be retrieved using direct approach as stated by [45] then the retrieval of SSS by using the availability of ocean colour data in the GIOVANNI’s web are challenges. Therefore, the primary objective of this study are (1). to develop an empirical model for relatively wider areas of the Banda Sea to estimate of SSS using of those data; (2). To assess how accurate the developed empirical model in estimating the SSS in the Banda Sea itself and from more global Indonesian waters.

2. Methodology

2.1. Study Area

This study conducted in the Banda Sea (121º to 134º E and -9º to -2º S), one of the inner seas in the Indonesian territory. Banda Sea bounded in the east by islands of Watubela, Kai, Tanimbar (Maluku Province); in the south by Islands of Wetar, Babar Lembata and Flores islands (Maluku and East Nusa Tenggara/NTT Provinces); in the west by islands of Wakatobi and around Kendari waters (Southeast Sulawesi Province); and in the north by islands Sulu, Buru and Seram North Maluku and Maluku

Provinces) [51, 52]. The Banda Sea is an important oceanographic link that connects the warm low salinity surface water from the Pacific to the Indian Ocean through several straits known as Indonesian throughflow (ITF) and then injected into the global ocean circulation system [53, 54].

2.2. Collection of SSS data

In this study, we selected only the field measurements of near-surface salinity and temperature from several oceanographic cruises that we attended using Research Vessel of Baruna Jaya (R/V BJ) VII and VIII and other field surveys, also from other sources (the National Oceanographic Data Center/NODC, National Oceanic and Atmospheric Administration/NOAA), such as Instant Cruise of RVBJ III, and from three Argo floats (Figure 1).

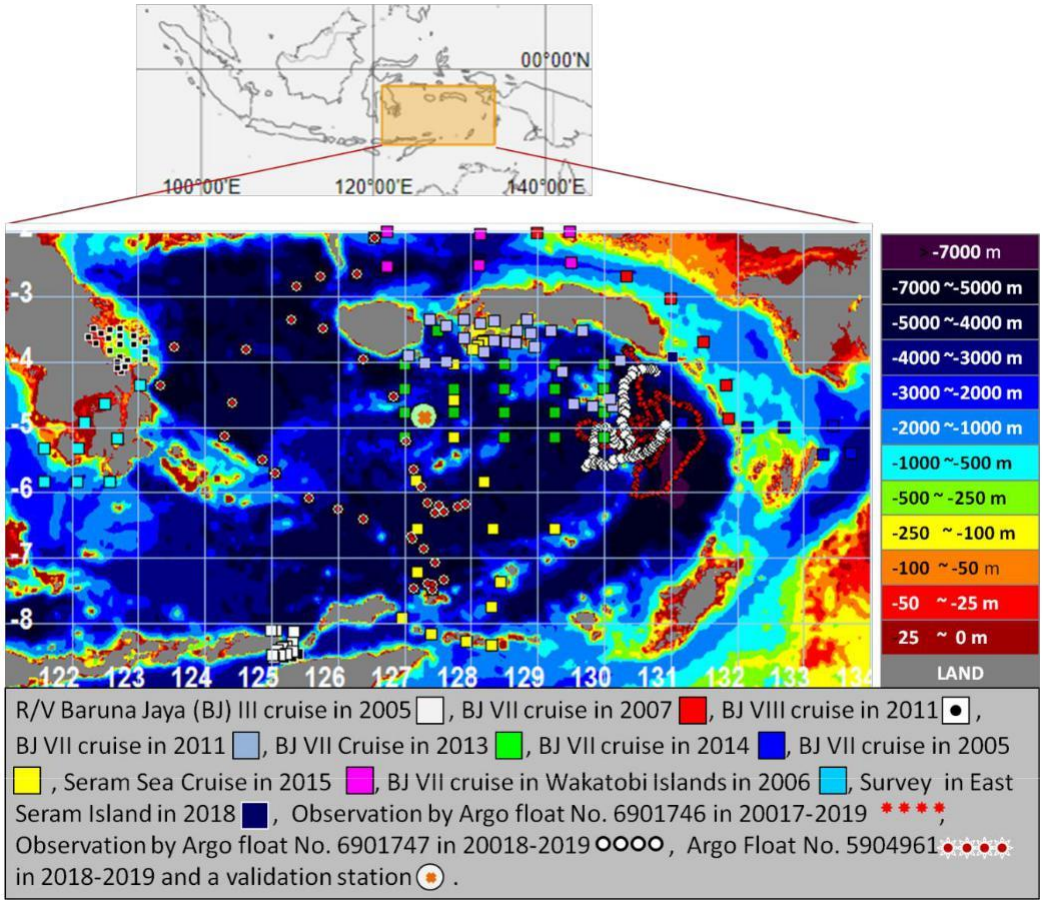

Figure 1. Map of Banda Sea showing the bathymetry and salinity measurement sites from various cruises, Argo floats and field surveys.

All of SSS data were collected from CTD cast using SBE9/11 Plus before 2012 and SBE19 Plus after 2012, except for field survey in the east Seram Island that used a small portable CTD (Table 1). The measured SSS data were not really in the sea surface, but rather in a deeper layer, about 1 to 4 m depth for data collected using CTD in all cruises and about 4 to 6 m for SSS data collected by Argo floats. Nevertheless, we categorized the near-surface salinity as SSS based on equation 1, which converts the salinity of Argos floats at 6 m depth to SSS in the surface layer (1 to 4 m). For example, salinity ranges of 33-34 PSU measured by Argo float at a depth of 6 m can be converted to the depth of 1-4 m by equation 1 with a result of salinity in the ranges of 32,987 ~ 33,997 PSU or with small differences of 0.013 ~ 0.003 PSU. Therefore, we use all directly CTD and Argo float measurement of the depth of 4 – 6 m as surface salinity (SSS).

$$SSS = 1.0099 \times \text{Salinity at depth 6 m} - 0.3401 \ (R^2 = 0.99); \ldots\ldots\ldots\ldots 1)$$

2.3. Satellite data used

Ocean color remotely sensed data used in this study were from the GIOVANI's web (https://giovanni.gsfc.Nasa.Gov/) from 2003 to 2019 with a spatial resolution of 4 km, while the temporal resolution of 8-daily. This web consists of 8 discipline fields, which two of them, the marine biologyand oceanography is closely related to this research, while each discipline has about 59 and 62 parameters. Among of those parameters, we selected 14 main parameters, namely remote sensing reflectance (Rrs) at 412, 433, 469 and 488 nm (Blue band), 531, 547, and 555 (Green band), and 645, 667 and 678 nm (Red bands). We also used data of the absorption coefficient of non-algae material due to detrital and CDOM material (ADG) at 443 nm; absorption coefficient due to phytoplankton (APH) at 443 nm, Chlorophyll-a concentration, and SST. All these data acquired from Aqua-MODIS satellite.The last two parameters together with the SSS that estimated from the empirical model developed in this study were latterly used for analysing the seasonal upwelling that occurs in the Banda Sea. The units of 14 ocean color parameters for Rrs, ADG / APH, Chl-a, and SST are sr^{-1}, m^{-1}, $mg.m^{-3}$, and ºC, respectively. All these downloaded data from the Giovanni web were carried out on the same date as the in-situ SSS measurements in the Banda Sea on an 8-daily basis. For example, cruise of RV BJ VIII to Kendari waters (Banda Sea) measures oceanographic parameters including SSS at 21 stations from 9-16 October 2011 (Table 1). Therefore, those 14 ocean color parameter data were taken in the same 8-daily time frame with the SSS field measurements (9 to 16 October 2011). Those 14 ocean color data of Rrs, ADG, APH, and SST are downloaded from Giovanni's web, then each data from the same position with 21 in-situ SSS measurement were extracted.

Table 1. Detailed SSS data collection used in this study

No.	Date	Cruise or Survey Name	Conducted by	# Stn
1.	Aug 8, 2003	Southern surveyor	Australia	3
2.	Jun 2-jul 29, 2005	RV/BJ III Instant Cruise 2005	Indonesia-CISRO, Australia	14
3.	Apr 16-22, 2006	RV/BJ VII KTI Cruise 2006 to Wakatobi Islands	Center for Deep Sea Research – LIPI, Ambon	9 of 24*
4.	Mar 3-23, 2007	RV/BJ VII Widya Nusantara Cruise 2007 to Misol Islands	Center for Deep Sea Research – LIPI, Ambon	6 of 30*
5.	Mar 27-Apr 5, 2011	RV/BJ VII Fish stock assessment Cruise 2011 to Banda Sea	Marine Affairs and Fisheries of Indonesia and Center for Deep Sea Research – LIPI, Ambon	16
6	Oct 9-16, 2011	RV/BJ VIII Cruise 2011 to Kendari waters	Research Center for Oceanography - LIPI, Jakarta	21
7	Nov 22-29, 2013	RV/BJ VII Banda Sea Expedition Cruise 2013	Center for Deep Sea Research – LIPI, Ambon	23
8	Mar 2-4, 2014	RV/BJ VII Cruise 2014 to Aru Islands	Center for Deep Sea Research – LIPI, Ambon	8
9	May 14-17, 2015	RV/BJ VII Cruise 2015 to Seram Sea	Center for Deep Sea Research – LIPI, Ambon	6
10	Nov. 9-19, 2015	RV/BJ VII Banda Sea Expedition Cruise 2015	Center for Deep Sea Research – LIPI, Ambon	20
11	Aug 2017 ~ now	Argo Float # 6901746**)	Faculty of Fisheries and Marine Sciences (IPB) and IFREMER, France	248
12.	Nov. 27-28, 2018	Survey in the east of Seram Island	Center for Deep Sea Research – LIPI, Ambon	5
13	Sep 2018 ~ now	Argo Float # 6901747***)	Faculty of Fisheries and Marine Sciences,IPB and IFREMER, France	84
14.	Jan-Des, 2018	Argo Float # 5904961****)	???	37

Remaks : *) 9 of 24 means only 9 stations of SSS measurements in the Banda Sea out of 24 stations. **) Argo float deployed 2017-07-14, Active (https://www.jcommops.org/); ***) Deployed in 2018-09-04. Inactive (https://www.jcommops.org/). ****) Deployed in 2016-06-23; Inactive (https://www.jcommops.org/).

2.4. SSS algorithm development and validation

In this study, we used simple regression analysis between SSS data collection from various cruises, field survey and Argo floats as listed in Table 1, and correlated them with 14 parameters of ocean color data extracted from Giovanni's web. Because data collected from all cruises and field surveys are not so many, only 75 datasets, then we used all these data to develop the SSS empirical model including SSS data measured by 3 Argo floats, but due to Argo floats data are many (n=177), then we selected only odd dates data (dates 1, 3, 5, .. 29, 31). The remaining even dates data (n=192) (dates 2, 4, 6, .. 28, 30) are stored for validating purposes (Table 2).

During the SSS empirical model development, several regression equation types such as exponential, linear, logarithmic, polynomial, and power regressions are tested. The initial curve fitting shows that the polynomial regression equation order 5 gives the best result with a high coefficient determination of R^2. Therefore, this type of equation is used.

Table 2. Three argo floats used for developing and validating the empirical SSS estimation model

Month and Year	Argo Float No. 6901746			Argo Float No. 6901747			Argo Float No. 5904961		
	Odd dates	Even dates	Total	Odd dates	Even dates	Total	Odd dates	Even dates	Total
Aug-17	10	16	26	-	-	-	-	-	-
Sep-17	11	13	24	-	-	-	-	-	-
Oct-17	16	-	16	-	-	-	-	-	-
Nov-17	-	11	11	-	-	-	-	-	-
Dec-17	-	11	11	-	-	-	-	-	-
Jan-18	n.a	n.a	n.a	-	-	-	2	-	2
Feb-18	-	10	10	-	-	-	3	-	3
Mar-18	-	10	10	-	-	-	3	1	4
Apr-18	13	-	13	-	-	-	4	-	4
May-18	14	-	14	-	-	-	4	-	4
Jun-18	-	15	15	-	-	-	-	1	1
Jul-18	-	11	11	-	-	-	-	4	4
Aug-18	13	-	13	-	-	-	4	-	4
Sep-18	-	9	9	11	-	11	-	3	3
Oct-18	-	15	15	15	-	15	-	3	3
Nov-18	11	-	11	-	15	15	4	-	4
Dec-18	13	-	13	-	15	15	1	-	1
Jan-19	-	15	15	14	-	14	-	-	-
Feb-19	11	-	11	-	14	14	-	-	-
Total	112	136	248	40	44	84	25	12	37

In order to examine the accuracy of our empirical model, the root mean square error (RMSE) expressed as Equation 2 is applied:

$$RMSE = \sqrt{\frac{1}{n}\sum_{i=1}^{n}(xi - \mu i)^2} \quad \ldots\ldots\ldots\ldots\ldots 2)$$

where n is Number of observation, xi and μ are true measurement and estimated values of SSS, respectively. Our empirical algorithm is also validated using multi-temporal SSS data obtained from Aquarius satellite at a point roughly in the mid-Banda Sea from 2012 to 2015. We used these data assuming that the accuracy in estimating SSS of this satellite is very high in the tropical open sea waters with RMSE of 0.2 PSU as expected when this satellite was launched [2, 18]

In addition, we extended our validation into 3 regions (Figure 2): (1) in the north of the Cendrawasih Bay and head of bird of Papua waters using Argo float # 5904515 and in the Halmahera and Maluku Seas using Argo Float # 5904508, which apparently influenced by south Pacific water masses; (2) In the South of Java to East Nusa Tenggara (NTT) waters using Argo floats # 5905014; 5905017 and 5904994; and Triumph Cruise of Training/RV of Madidihang II in 2018 that conducted by Research Center for Deep Sea (P2LD LIPI) Ambon, Indonesia, First Institute of Oceanography

(FIO), China and Maryland University, USA; (3) West of Sumatra Island near to Enggano Island using Argo Float # 5904723, Mentawai Islands using Argo Float # 1901441 and Sabang Island, North Aceh using Argo float # 1901442. Region 2 and 3 are influenced by the Indian Ocean water masses. Thus, the purpose of this validation is to confirm whether the empirical model of SSS developed for the Banda Sea can be applied or not for all Indonesian waters.

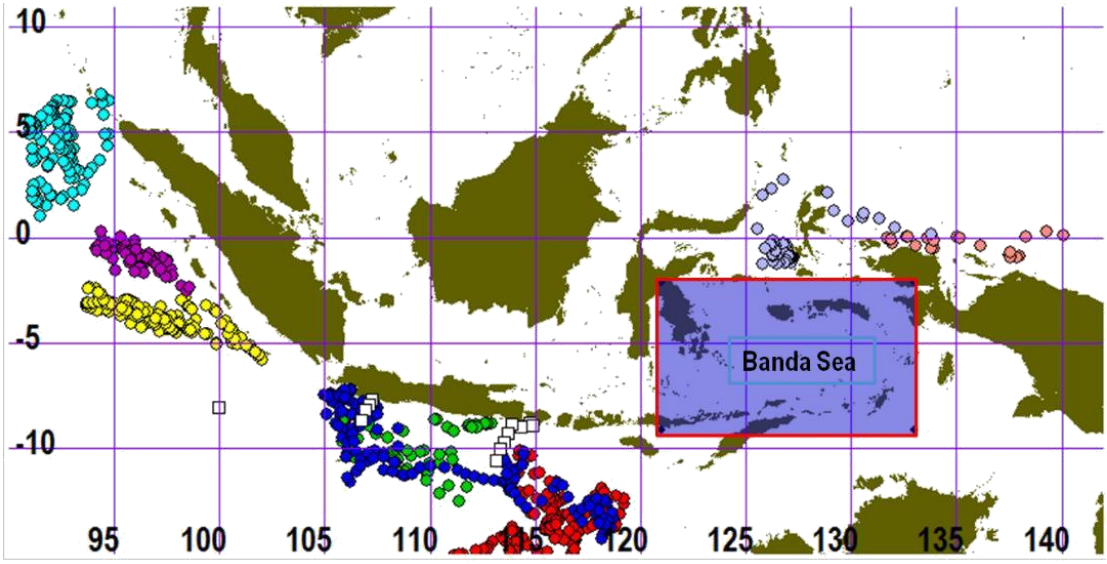

Figure 2. Validation of SSS empirical model of the Banda Sea (map in the the box) using: A). Argo floats # 5904515( ) and # 5904508 ( ) of the north Cendrawasih Bay and head of bird of Papua and Halmahera and Maluku Seas, respectively that was under influenced by south Pacific water masses; B) Argo floats # 5905014 ( ), # 5905017 ( ), # 5904994 ( ) and Triumph Cruise ( ), which was under influenced by Indian Ocean water masses of south Java and NTT; and C). Argo floats # 5904723 ( ), # 1901441 ( ) and # 19014442 ( ), which was under influenced by Indian Ocean water masses of west Sumatera.

.

3. Results and Discussion

3.1. In situ SSS data measurements and their distribution

The overall SSS *in situ* measurements of various cruise ships, Argo buoys and surveys conducted in the Banda Sea from 2003 to 2018 show that the minimum, maximum, mean and standard deviations of the SSS are 30.425, 34.532, 33.781, and 0,233 PSU (Table 3). The distribution of SSS from a cruise in Kendari waters (inner and outer Lasolo Bay and Kendari Bay) during October 2011 was the most varies than other places due to the influence of the freshwater coming from the nearby river around the bay. The SSS ranges from 30,425 ~ 34,007 PSU with a mean value of 33,095 PSU and the highest standard deviation value of 1.017 PSU. On the other hand, the Banda Sea cruise-2 on Nov. 9-19, 2015 measured relatively higher SSS in the ranges of 34.263 to 34.532 PSU with a mean value of 34.384 PSU and low standard deviation of 0.101 PSU. The three Argo floats measured the same high values of SSS in the ranges of 33.844 to 34.257 PSU with a mean value of 34.175 PSU and a standard deviation of 0.130 PSU from August 2017 to December 2018 (Table 3). From all SSS measurements listed in Table 3, the value of SSS not exceed 34.6 PSU, which shows that the Banda Sea is affected by warm-low salinity of the upper layer (0-250 m) of Pacific Ocean water masses [53, 54].

If all in-situ SSS data in Table 3 (left) are classified accordingly to 4 local seasons, namely the Northwest monsoon (December-February; DJF), Transition Season-I (March-May; MAM), Southeast monsoon (June-August; JJA) and transition-II season (September -November; SON) (Table 4), it can be seen that the average SSS value during the DJF was relatively high at 33,985 PSU, but decreased to 33,471 PSU in MAM due to the influence of rainfall during the DJF until the end of MAM, but increased again to 33,929 PSU in JJA, and reaches its peak during SON with SSS value of 34.059.

Table 3. SSS measured from various cruises, Argo floats and field survey in the Banda Sea from 2003 to 2018

No.	Date	Cruise or Survey Name	N.	Min.	Max.	Mean	Std.
1.	Aug 8, 2003	Southern surveyor	3	34.246	34.250	34.248	0.002
2.	Jun 2-Jul 29, 2005	RV/BJ III Instant Cruise 2005	14	33.776	33.882	33.877	0.038
3.	Apr 16-22, 2006	RV/BJ VII KTI Cruise to Wakatobi Islands	9	32.674	33.360	32.972	0.344
4.	Mar 3-23, 2007	RV/BJ VII Widya Nusantara Cruise 2007	6	33.194	34.113	33.618	0.364
5.	Mar 27-Apr 5, 2011	RV/BJ VII Fish stock assessment Cruise	16	32.788	33.701	33.208	0.306
6	July 10-19, 2011	RV/BJ VIII Cruise Kendari waters 2011	21	30.425	34.007	33.093	1.017
7	Nov 22-29, 2013	RV/BJ VII Banda Sea Expedition Cruise-1	23	33.628	34.048	33.935	0.113
8	Mar 2-4, 2014	RV/BJ VII Cruise 2014 to Aru Islands	8	33.619	33.987	33.772	0.157
9	May 14-17, 2015	RV/BJ VII Cruise 2015 to Seram Sea	6	33.299	33.816	33.653	0.212
10	Nov. 9-19, 2015	RV/BJ VII Banda Sea Expedition Cruise-2	20	34.263	34.532	34.387	0.101
11	Aug 2017 ~ now	Argo Float # 6901746**)	248	33.844	34.414	34.127	0.176
12.	Nov. 27-28, 2018	Survey in the east of Seram Island	5	33.885	34.055	33.999	0.051
13	Sep 2018 ~ now	Argo Float # 6901747	84	34.107	34.412	34.257	0.074
14	Jan-Des, 2018	Argo Float # 5904961	37	33.973	34.272	34.140	0.140

Table 4. Seasonal mean in-situ SSS of the Banda Sea based on data in the Table 3.and averaged seasonal rainfall rate from 2003-2018

Season	SSS (PSU)				Rainfall rate (mm.hour^{-1})			
	Min.	Max.	Mean	Std	Min.	Max.	Mean	Std
Northwest monsoon (DJF)	33.846	34.130	33.985	0.100	0.114	0.547	0.314	0.063
Transition season-1 (MAM)	33.138	33.815	33.471	0.256	0.091	0.703	0.290	0.092
Southeast monsoon (JJA)	33.318	34.230	33.929	0.245	0.011	0.746	0.176	0.117
Transition season-II (SON)	33.829	34.244	34.059	0.129	0.030	0.371	0.108	0.067

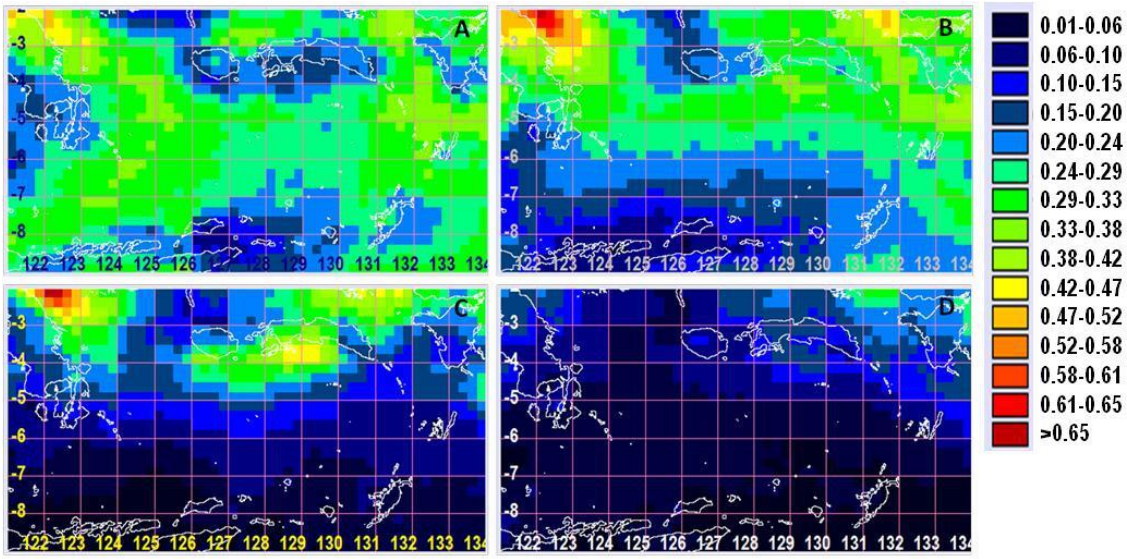

Figure 3. Mean precipitation rate (mm.hour^{-1}) map of Banda Sea from 2003-2018. (A). DFJ, (B) MAM, (C) JJA, (D) SON.

Figure 3 displays the same four seasons (DJF, MAM, JJA, and SON) of mean monthly precipitation rate (mm/hour) of the Banda Sea from 2003 to 2018 produced using microwave-infrared satellite by the Tropical Rainfall Measuring Mission (TRMM) of NASA and JAXA (Japan Aerospace Exploration Agency). It is also shown that the average rainfall rate in the entire Banda Sea from the highest to the lowest values are in the DJF, MAM, JJA and SON seasons with values of 0.31, 0.29, 0.18 and 0.11 mm.hour^{-1}, respectively. The rainfall rate inversely affects the seasonal variability of

SSS. For example, high rainfall rate at the DJF-MAM correlates with lower SSS. On the other hand, lower rainfall rate at JJA and SON causes the SSS to be higher (Table 4). However, different local climate variations between the northern and southern Seram Islands include Ambon Island and Lease Islands (126-131 E; 3-4.5 S), especially in the DJF, MAM and JJA seasons (Figures 3a, 3b, and 3c) can be affected the local SSS distribution patterns in both locations. For example, the results of the study [55] on the SSS of Ambon Bay that was under the influence of the Banda Sea showed different results with our study. They found a maximum SSS value of 34.96 PSU in July, which had heavy rainfall during that month (Figure 3c), but the same result with us for the minimum SSS value of 33.50 PSU in April.

3.2. Empirical SSS Model Development and Validation

The empirical SSS Model was developed by using a simple regression equation between measured SSS data from all cruises, Argo floats and field survey and ocean colour data acquired from Aqua-MODIS satellite in the forms of Remote Sensing Reflectance (Rrs) data of Blue, Green and Red bands (sr^{-1}), ADG at 443 nm; (m^{-1}), and APH at 443 nm (m^{-1}) that summarized in Table 5. All of these ocean colour data were provide by Giovanni NASA's web. The data in Table 5 generally shows that the range, mean values, and standard deviation values of each Rrs in the blue spectral bands is the highest followed by the green spectral band and the spectral red band as the lowest, while the average value of all Rss of blue, green and red bands have the same pattern as previous. The mean value for APH 443 nm, is higher than the ADG 443 nm.

Table 5 summarizes the ocean color parameter data used in the development of the SSS estimation empirical model Blue bands

Ocean color parameter		Min	Max	Mean	Stdev
Blue bands	Rrs-412	0.0014	0.0124	0.0072	0.0028
	Rrs-443	0.0029	0.1599	0.0142	0.0232
	Rrs-469	0.0030	0.0085	0.0057	0.0016
	Rrs-488	0.0028	0.0070	0.0050	0.0012
Green bands	Rrs-531	0.0018	0.0085	0.0028	0.0009
	Rrs-547	0.0015	0.0031	0.0020	0.0003
	Rrs-555	0.0012	0.0085	0.0030	0.0024
Red bands	Rrs-645	0.0005	0.0041	0.0002	0.0005
	Rrs-646	0.0004	0.0037	0.0002	0.0005
	Rrs-647	0.0003	0.0036	0.0002	0.0004
Mean Rrs Blue bands		0.0031	0.0438	0.0081	0.0056
Mean Rrs Green bands		0.0016	0.0047	0.0026	0.0009
Mean Rrs Red bands		0.0004	0.0038	0.0002	0.0005
ADG at 443 nm		0.0051	0.1320	0.0175	0.0212
APH at 443 nm		0.0097	0.1599	0.0236	0.0221

To develop the empirical model of SSS, we tested several types of regression equations such as linear exponential, logarithmic, polynomial and power using curve fitting. The initial results show that the polynomial regression order 5 gives good performance with the highest coefficient determination (R^2). Therefore, this regression type was used as empirical model to estimate the SSS from ocean color data.

Table 6 displays the R^2 values of polynomial regression order 5 between SSS and Rrs of Blue band (412, 443, 469 and 488 nm), Green band (531, 547 and 555 nm) and Red band (645, 667 and 678 nm) including their transformation, such as the mean Rrs of Blue, Green and Red Bands; The mean Rrs of Chromaticity Blue (B/(B+G+R)), Green (G/(B+G+R)) and Red (B/(B+G+R)), the mean Rrs of Ratio Blue to Green (B/G), Blue to Red (G/R) and Green to Red (G/R). The ADG at 443 nm produces the highest R^2 (0.94), followed by mean Rrs of blue chromaticity (R^2= 0.92), mean Rrs of Ratio B/G R^2=0.90), mean Rrs of Green chromaticity (R^2= 0.84), and APH at 443 nm (R^2= 0.84), while R^2 of Rrs parameters and their other transformation < 0.70.

Table 6. Coefficient Determination (R^2) resulted from polynomial order 5 regression analysis between SSS and Rrs of Blue, Green and Red bands and their transformation.

Remote Sensing Reflectance (Rrs)	Blue Bands				Green Bands			Red Bands		
	Rrs-412	Rrs-443	Rrs-469	Rrs-488	Rrs-531	Rrs-547	Rrs-555	Rrs-645	Rrs-646	Rrs-647
	0.60	**0.66**	**0.05**	**0.03**	**0.45**	**0.034**	**0.05**	**0.61**	**0.61**	**0.62**
Mean of all Rss	Blue: **0.58**				Green: **0.11**			Red: **0.56**		
Mean of Rrs Chromaticity (Chr.)	Chr. Blue: **0.92**				Chr. Green: **0.84**			Chr. Red: **0.30**		
Mean Rss Ratio	Blue/Green : **0.90**				Blue/Red: **0.05**			Green/Red: **0.37**		
ADG at 443 nm	**0.94**				-			-		
APH at 443 nm	**0.84**				-			-		

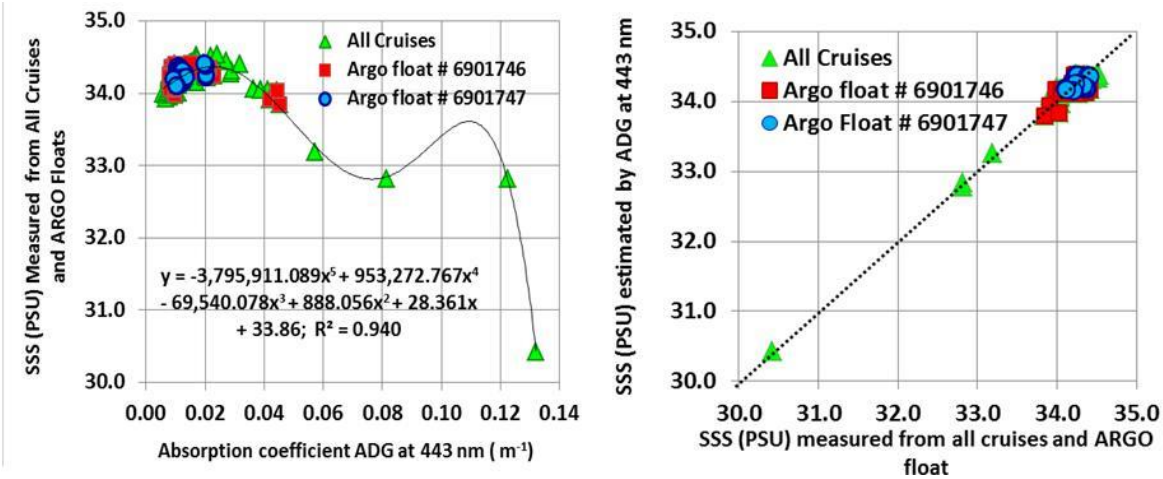

Figure 4. Plot of ADG at 443 nm versus SSS measured from Cruises, Argo floats and field survey (Left side); Performance of this empirical model in retrieving SSS (right side).

Since ADG at 443 nm gives the highest R^2 values then we select this parameter for estimating the of the Banda Sea. Figure 4 left side show plot between ADG at 443 nn against in-situ SSS measurements from the various cruises, Argo float, and field survey data (Table 1), while Figure 4 right side displays performance of this empirical model in retrieving SSS. The SSS empirical model in Figure 4 can be rewritten as expressed in the equation 3 bellow:

$$SSS = 3785911.089*X^5+953272.767*X^4–69540.078*X^3+888.056*X^2+28.361*X+33.860 \quad \ldots\ldots 3)$$

Where X = absorption coefficient of ADG at 443 nm. Figure 4 (right side) indicates that the SSS estimated using ocean color parameter of the ADG 443 follows a 1: 1 line with high accuracy and with a small root mean square error (RMSE) of 0.103 PSU as shown in Table 7 within the SSS ranges of 30.42-34.53 PSU. However, accuracy assessment using the Argo floats #6901746 and #6901747 data that measured SSS in the even dates in the eastern part of the Banda sea (Figures 1) show a slightly higher RMSE value of 0.369 and 0.234 PSU (Table 7), respectively, but the comparison with SSS retrieved from Aquarius satellite data in the mid of the Banda Sea (Figures 1) shows significantly low RMSE value of 0.145 PSU (Table 7). This value is smaller than 0.2 PSU, which indicates that the accuracy of our empirical models to estimate the SSS is equal the expected accuracy of Aquarius satellite in measuring the global SSS as a prerequisite when this satellite launched (RMSE 0.2 PSU) [2, 18]. However, the accuracy of this model becomes slightly lower if compared to the above two Argo floats.

Table 7. Accuracy of the empirical model in term of RMSE for estimating the SSS within and outside the Banda Sea

No.	Observation by	Location	Dates	N	in Situ SSS (PSU)		Predicted SSS (PSU)		RMSE
					Min	Max	Min	Max	
Within the Banda Sea									
1	**All Cruise + Argo float**	**All Banda Sea**	**Aug 2003 - Feb 2019**	**141**	**30.425**	**34.532**	**30.427**	**34.378**	**0.101**
2	Argo float #6901746	East Banda Sea	Aug 2017 - Feb 2019	196	33.253	34.494	33.779	34.378	0.369
3	Argo float #6901747	East Banda Sea	Nov 2018 - Feb 2019	40	34.014	34.447	34.069	34.231	0.234
4	Aquarius Satellite	Mid Banda Sea	Sep 2011 - Jan 2012	11	34.001	34.470	34.048	34.346	0.145
Outside the Banda Sea									
5	Argo float #5904515	Cendrawasih Bay	Oct 2018 - May 2019	19	33.984	34.661	34.000	34.375	0.297
6	Argo float #5904508	Maluku Sea	Nov.2017 - Apr 2019	73	32.613	34.393	33.860	34.359	0.501
7	Argo float #5905014	Banyuwangi-Bali	Jan 2016 - Sep 2018	33	33.721	34.917	33.987	34.364	0.503
8	Argo Float #5905017	Nusa Kambangan	May 2017 - May 2019	55	32.622	34.515	34.022	34.376	0.555
9	Triumph Cruise	Sourthern Java	Oct 2018	9	34.188	34.514	33.824	34.310	0.343
10	Argo float #1901442	Sabang Isl.	Sep 2013 - May 2019	55	32.051	34.904	33.993	34.360	0.553
11	Argo float #1901441	Mentawai Isl.	Sep 2017 - May 2019	57	33.164	34.903	33.892	34.200	0.384
12	Argo float #5904723	Enggano Isl.	Apr 2016 - May 2019	102	32.963	34.761	33.860	34.264	0.360

Table 7 displays also the RMSE of this empirical model to estimate the SSS outside the Banda sea, which under the influenced of the Pacific Ocean water masses and Indian Ocean water masses of the southern the Java-Bali Islands and of the western of the Sumatra Island (Figure 2). The accuracy of this model is lower when it is used to estimate SSS in waters outside the Banda Sea. For the water mass under the influence of the Pacific Ocean, the RMSE produced by this model were 0.277 and 0.510 for the Cendrawasih Bay and the Maluku Sea, respectively. RMSE For waters under the influence of Indian Ocean in the south of Java and Bali Islands were 0.343 (Truimph Cruise 2018), 0.503 PSU (Banyuwangi-Bali) and 0.555 PSU (around Nusa Kambangan waters), while the RMSE for waters under the influence of the same Indian Ocean, but in the western of Sumatra Island was 0.340 PSU (waters near Enggano Island), 0.384 PSU (waters around the Mentawai islands), and 0.553 PSU (waters around Sabang Island, Aceh).

Although this empirical model has high accuracy in estimating SSS (within a range of 30,427 ~ 34,378 PSU; RMSE 0.101 PSU), but the analysis of SSS estimation accuracy based on RMSE results for various locations both within the Banda Sea and outside the Banda Sea (Table 7) shows that this model actually can predict in-situ SSS with high accuracy only in a narrow range of 33.5-34.5 PSU, such as the comparison result between the SSS of this model and SSS measured by Aquarius satellite (SSS: 34.001~34.470 PSU; RMSE: 0.145 PSU, and in around of the Cendrawasih Bay (SSS: 33.984~34.661 PSU; RMSE: 0.297 PSU). The bias becomes higher when in-situ SSS <33.5 PSU (such as in the Maluku Sea, SSS: 32.613~34.393 PSU, RMSE: 0.501 PSU, and Nusa Kambangan waters, SSS: 32.622~34.515 PSU, RMSE: 0.555 PSU) or >34.5 PSU (such as in Banyuwangi-Bali waters, SSS: 33.721~34.917 PSU, RMSE: 0.503 PSU, and Sabang Island waters, SSS: 32.051~34.904 PSU; RMSE: 0.553 PSU). Nevertheless, this empirical model has limitations in estimating in-situ SSS with high accuracy only in a narrow range, but the model at least showed reasonably good performance to retrieve the SSS data and information not only in the Banda Sea, but also in the most of Indonesian waters.

As a comparison with this study, Table 8 presents some SSS estimation using ocean color data derived from Aqua-MODIS and GOCI satellites from various study. These results indicate that ocean color data with different wavelength bands (both for land [57,58], and sea applications [44,56,57,6] or their combination [17] of MODIS sensor) as well as various methods including, neural network [56,5717], band ratios [44, 6] can be directly used to predict and to map SSS without using the CDOM-salinity approach first [37, 38, 28, 39, 24, 31, 40, 41, 42, 43 29, 3, 15,44,5], as stated by [45]. Our study also indicates that the ratio of Rrs Blue to Green and Rrs Chromaticity of Green (Green/(Blue+Green+Red)) has a high relationship with SSS of R2=0.90 and 0.84, respectively (Table 6). However, the ADG parameter, which is the non-phytoplankton detrital material or CDOM absorption coefficient at a wavelength of 443 has the highest R^2 (0.94) and thus used to predict the SSS directly. Thus, Table 8 concludes that ocean color optical satellites such as MODIS and/or GOCI have a great potential to provide data and information about SSS and to map it.

Table 8. SSS derived from Aqua MODIS and GOCI satellites using various wavelength bands and various algorithms as a comparison with this study.

No.	Location	Satellite and model used to estimate SSS	Salinity (PSU)	R^2	RMSE	Source
1	Bohay Sea, China	Aqua-MODIS, Band Ratio, Rrs (531) / Rrs (555)	28~31	0.76	0.26	[44]
2	Gulf of Mexico, USA	Aqua-MODIS, Neural Network, Input parameters Rrs (412, 443, 488, 555, and 667 nm) and SST	27~ 37	0.86	1.2.	[56]
3	Chesapeake Bay, USA	Aqua-MODIS, Neural Network, Input parameters Rrs (412, 443, 412/547, 443/547, 488/547 nm), Longitude, Latitude, and (SST).	9.58 ~ 32.7	0.98	1.12	[57]
4	Coast of Peninsular Malaysia	Aqua/Tera(?)-MODIS, Multiple regression analysis of the first seven bands (Band 1 ~ 7)* of MODIS	28.5 ~ 33.5	0.96	0.37	[58]
5	Hong Kong waters	Aqua-MODIIS, Multiple regression analysis of the first seven bands (Band 1 ~ 7)* of MODIS	10~34	0.81	1.63	[45]
6	Northern Gulf of Mexico, USA	Aqua-MODIS, Neural Network, input parameters Water leaving Reflectance Band (1,4)*, and Band (8,9, 10,14)**	10 ~ <35	0.90	N/A	[17]
7	Southern Yellow Sea, China	GOCI, Band ratio, Rrs (490) / Rrs(555) and; [Rrs(490)-Rrs(555)] / [Rrs(490)+Rrs(555)]	28-78 ~ 32.74	0.76 0.79	0.31 0.29	[6]
8	Banda Sea, Indonesia	Aqua-MODIS, ADG due to CDOM at 443nm	30.4 ~ 34.5	0.94	0.101	Ths study

Remarks : * Band 1-7 are MODIS Band for Land application; ** Band 8-16 are MODIS Bands for Ocean application

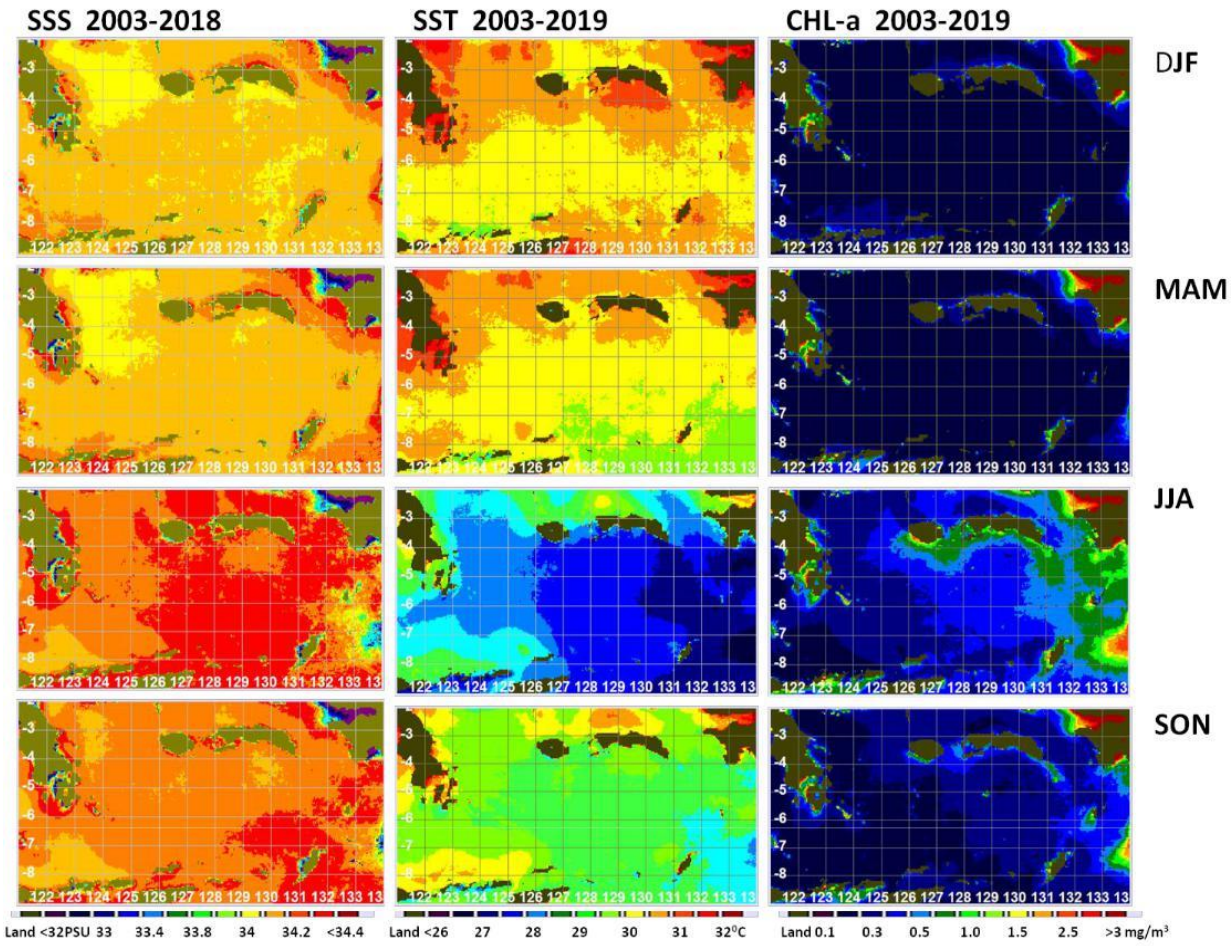

Figure 5. Mean climatological SSS, SST and Chl-a based on DJF, MAM, JJA and SON seasons from 2003-2018.

3.3. *Application of Empirical SSS Model to study the upwelling of the Banda Sea*

Figure 5 shows the mean seasonal climatological patterns of SSS, SST and Chlorophyll-a (Chl-a) concentrations from 2003-2018. These oceanographic parameters of the SSS generated from the empirical model in this study together with SST and Chl-a downloaded from the Giovanni's web shows very clearly the upwelling phenomenon occurred in the Banda Sea during the southeast monsoon from June to August (JJA), which indicated by relatively high value of SSS in the ranges of 1.000~34.374 PSU with an average of 34.189 PSU; by low SST value ranges of 26^0C ~ 30^0C with an average of 28^0C, and by higher Chl-a concentration ranges of 0.2~3.0 mg.m^{-3} with an average of 0.6 mg.m^{-3} compared with before upwelling during the northeastern monsoon (DJF) and the transition season I (MAM) as well as after upwelling during the transition season II (SON).

The upwelling phenomenon of this study (Figure 5) was very consistent with the results of our old upwelling study in the Banda and Seram Seas during the four cruises of R/V Soerjaatmadja that representing four seasons, May 1996 (MAM), August 1996 (JJA), November 1996 (SON) and January 1997 (DJF) [59]. Table 9 displays the average value of six oceanographic parameters measured at 33 stations from the surface to a depth of 50 m. Of the 4 cruises to the Banda Sea, the upwelling event in the Banda Sea occurred on August 1996 or during the Southeast monsoon (JJA) indicated by the values of high SSS (34.155~34.559 PSU), low SST (25.93~27.26^{o}C), high Chl-a concentration (0.39~1.14 mg.m^{-3}), low dissolved oxygen (DO) (3.34~4.10 ml/l), and high nutrients of nitrates (0.024~0.0087 mg/l) and phosphates (0.045~0.051 mg/l) compared to three other observation months. This old study showed that upwelling was in its final phase so that its intensity was weak as indicated by several oceanographic parameters such as Salinity, Chl-a, and DO not reveal clearly at sea surface, except at depths of 25 and 50 m (Table 9) [59]. Upwelling of the Banda Sea was assumed to be due to southerly-southeasterly strong winds that were blowing and bringing dry air that constantly during that season (JJA) [59, 60]. There was a time lag about 2-3 months from upwelling season to generate the phyto-zooplankton abundance and the formation of skipjack tuna fishing ground, especially around the Buru-Manipa-Kelang-Buano Islands of the Maluku Province [59, 60]. The results of other studies also confirm that upwelling in the Banda Sea occurs in the Southeast monsoon can cause temperature differences up to 4^{o}C cooler than the northeast monsoon The moving of deep water mass with a density of >22 kg/m^3 or with high salinity to shallower waters was also found during the southeast monsoon period, which associated with upwelling events in the Banda Sea [61]. This study also agrees well with [62] that stated the variability of the SST during the southeast monsoon (JJA) or upwelling season (26.0~29.5^{o}C) cooler than the northwest monsoon (DJF) (28.5~30.5^{o}C), while the SSS in this season fresher (33.0~34.5 PSU) than the upwelling season (34.25~34.75 PSU). The high concentration of Chl-a during upwelling (the southeast monsoon) also seems to be triggered by nutrient input from various rivers as a result of relatively higher rainfall rate in the northeast monsoon (DJF) until transition-1 (MAM) seasons as shown in Figure 3.

Table 9. Old upwelling oceanographic data conducted during four cruises of R/V Soerjaatmadja in the Banda Sea from May 1996 to January 2017 [59].

Depth (m)	May-96 (MAM)	**Aug-96 (JJA)**	Nov-96 (SON)	Jan-97 (DJF)	May-96 (MAM)	**Aug-96 (JJA)**	Nov-96 SON	Jan-97 (DJF)	May-96 (MAM)	**Aug-96 (JJA)**	Nov-96 SON	Jan-97 (DJF)
	SSS (PSU)				**SST (°C)**				**Chl-a (µg/l)**			
0	33.36	**34.155**	34.269	34.006	28.67	**27.26**	29.14	29.32	0.46	**0.39**	0.32	0.35
25	33.84	**34.559**	34.307	34.092	28.49	**26.71**	28.06	28.65	0.51	**0.66**	0.58	0.50
50	34.105	**34.558**	34.387	34.129	27.54	**25.93**	27.06	28.46	0.53	**1.14**	0.74	0.58
	DO (ml/l)				**Nitrate (mg/l)**				**Phosphate (mg/l)**			
0	4.52	**4.10**	4.14	4.00	0.011	**0.024**	0.011	0.011	0.029	**0.045**	0.031	0.026
25	4.36	**3.61**	4.03	3.95	0.014	**0.054**	0.024	0.010	0.031	**0.047**	0.028	0.024
50	3.94	**3.34**	3.67	3.84	0.027	**0.087**	0.037	0.012	0.038	**0.051**	0.029	0.027

Concluding Remarks

This study analyzes the potential of Aqua-MODIS ocean color satellite imagery to estimate SSS through the development of empirical models and assesses the accuracy of this model. The Rrs and ADG at 443 nm data available on the NASA Giovanni website are proven to be directly used (without going through the CDOM-Salinity approach) to predict SSS not only for the Banda Sea but for most Indonesian waters with high accuracy, although still limited to a narrow SSS range between 33.5 PSU

and 34.5 PSU. Therefore, it is necessary to develop and to validate this empirical model, which able to predict the SSS throughout the Indonesia waters with wider SSS range, and higher spatial resolution (1 km) of Aqua-MODIS data. The SSS products developed from this study together with other data such as SST, Chl-a and/or other marine remote sensing data can describe many other topics on oceanography fields in more depth such as the upwelling study as discussed in this study.

Acknowledgments

The authors wish to thank to the Director of Research Centre for Deep Sea (P2LD-LIPI), Ambon (Dr. Augy Syahailatua and his staffs, Widya N. Satrioadjie, Terry Indrabudy and Daniel Pelasula) for financial support and helping us to participate in MSAT 2019 program. All Argo float data used in this study were collected and made freely available by the Coriolis project and programmes that contribute to it (*http://www.coriolis.eu.org)*. Analyses and visualizations used in this study were produced with the Giovanni online data system, developed and maintained by the NASA GES DISC.

References

[1] Pawlowicz R 2017 Encyclopedia of Sustainable Technologies, Vol.4:135-143 http://dx.doi.org/10. 1016/B978-0-12-409548-9.10157-513-5
[2] Zine S, Boutin J, Waldteufel P, Vergely J-L, Pellarin T and Lazure P 2017 *IEEE Transaction on Geosience and Remote Sensing*. Vol.45(7):2061-2072
[3] Geiger E F, Grossi M D, Trembanis A C, Kohut J T, and Olive M J 2011 *Continental Shelf Research* (2011), doi:10.1016/j.csr.2011.12.001
[4] Boutin J, Jean-Luc V, Marchand S, D'Amico F, Hasson A, Kolodziejczyk N, Reul N, Reverdin G and Vialard J 2018. *Remote Sensing of Environment*, Elsevier, 2018, 214, pp.115-134.10. 1016/j.rse.2018.05.022. hal-01844300.
[5] Nakada S, Kobayashi S, Hayashi M, Ishizaka J, Akiyama S, Fuchi M and Nakajima M 2017 *Journal of Oceanography* https://doi. org/ 10.1007/s10872-017-0459-4
[6] Sun D, Su X, Qiu Z, Wang S, Mao Z and He Y 2019 *Remote Sens*. 2019, 11, 775; doi: 10.3390/rs11070775
[7] Kantoussan J, Ecoutin J M, Simier M, de Morais L T and Laë R 2011. *Estuarine, Coastal and Shelf Science*, http://dx.doi.org/10.1016/j.ecss.2012.07.018
[8] Corbett C M 2016 *Utilization of Satellite-Derived Salinity for ENSO Studies and Climate Indicies*. Master Thesis in Geological Sciences, College of Arts and Sciences University of South Carolina. 65p.
[9] Corbett C M, Subrahmanyam B and Giese B J 2017 *Clim. Dynam*. **49** (9-10), 3513–3526, doi: 10.1007/s00382-017-3527-y
[10] Singh A, Delcroix T and Cravatte, S. 2011. *J. Geophys. Res.*, 116, C06016, doi:10.1029/ 2010JC006862.
[11] Hasson A, Delcroix T, Boutin J, Dussin R. and Ballabrera-Poy, J. 2014. *J. Geophys. Res. Oceans*,119, 3855–3867, doi:10.1002/2013JC009388
[12] Zhu J, Huang B, Zhang R-H, Hu, Z-Z, Kumar A., Balmaseda M A, Marx L and Kinter J L 2014 Salinity anomaly as a trigger for ENSO events. Scientific Report 4: 6821 DOI: 10.1038/ srep06821
[13] Du Y. and Zhang Y. 2015 *Journal of Climate*. Vol.15:695-713. DOI:10.1175/JCLI-D-14-00435.1
[14] Zhang Y, Du Yan and Qu T 2016 *Clim Dyn* 2016 47:2573–2585. DOI 10.1007/s00382-016-2984-z
[15] Wouthuyzen S, Tarigan S, Kusmanto E, Supriyadi H I, Sediadi A, Sugarin, Siregar V P and Ishizaka J 2011 *Mar. Res. Indonesia* Vol36(2):51–70
[16] Crapolicchio R, Ferrazzoli , Meloni M, Pinori S and Rahmoune R 2010 *Italian Journal of Remote Sensing*, 2010, 42(1):37-50

[17] Wang J and Deng Z 2018 *International Journal of Remote Sensing*, Vol. 39(11):3497–3511 https:// doi.org/10. 1080/01431161.2018.1445880
[18] Xia S, Ke C, Zhou X and Zhang J 2016 *Acta Oceanol. Sin*. Vol.35(3):54–62. DOI:10.1007/s13131-016-0818-9.
[19] Kao H Y, Lagerloef G S E, Lee T, Melnichenko O, Meissner T and Hacker P 2018 *Remote Sens*. 10, 1341; doi:10.3390/rs10091341
[20] Xie P, Boye R T, Bayler E, Xue Y, Byrne D, Reagan J, Locarnini R, Sun F, Joyce R and Kuma A *J. Geophys. Res. Oceans*, 119, 6140–6160, doi:10.1002/2014JC 010046
[21] Bhaskar U T V S and Jayaram, C 2015 *IEEE Geoscience and Remote Sensing Letters* February 2015 DOI: 10.1109/LGRS.2015.2393894
[22] Tong X, Wang Z and Li Q 2015 *Chinese Journal of Oceanology and Limnology* Vol. 33 (4):1072-1084, http://dx.doi. org/10.1007/s00343-015-4196-5 ,
[23] Aksoy M and Johnson J T 2013 *IEEE T. Geosci. Remote*, 51 (10), 4983-4992, doi: 10.1109/ TGRS.2013.2266278
[24] Ahn Y H, Shanmugam P, Moon J E and Ryu J H 2008 *Annales Geophysicae*, Vol.26 (7):2019–2035.
[25] Del Castillo C E and Miller R I 2008 *Remote Sensing of Environment*, 112:836–844
[26] Jerlov, N. G. 1968. *Optical oceanography*. Amsterdam: Elsevier. 194 pp.
[27] Monahan E C and Phybus M J 1978 *Nature*, 274:782–784
[28] Binding C E and Bowers D G 2003 *Estuarine Coastal and Shell Scince*, 57:605–611.
[29] Hu C, Chen Z, Clayton T D, Swazenski P, Brock J C and Muller-Karger F E 2004. *Remote Sensing of Environment*, 93 : 423–441
[30] Chen Z, Hu C, Comy R N, Muller-Karger F E and Swarzenski P 2007 *Marine Chemistry*, 104:98–109.
[31] Bowers D G. and Brett. H L 2008 *Journal of Marine Systems*. 73: 1–7.
[32] Shank G C, Nelson N and Montagna P A Estuary. *Estuary and coasts*,32:661–667.
[33] Maul, G.A. 1985. *Introduction to satellite Oceanography*. Martinus Nijhoff Publisher. 606 pp.
[34] Fischer, J. and U. Kronfeld, 1990. Sun-simulated chlorophyll fluorescence: Influence of oceanic properties. *Int. J. Remote Sensing*. 11(12):2125–2147.
[35] Kirk J T O 1994 *Light and Photosynthesis inAquatic Ecosystem*. Cambridge University Press. 509 pp.
[36] IOCCG 2000 Sathyendranath, S.(*ed*), *Report of the International Ocean-Colour Coordinating Group*, No.3. IOCCG, Dartmouth, Canada.
[37] D'Sa E J, Hu C, Muller-Karger F E and Carder K L 2002 *Proc. Indian Acad. Sci. (Earth Planet. Sci.),* 111 (3): 197–207.
[38] Hu C, Muller-Karger F E, Biggs D C, Carder D C, Nababan B, Nadeau D and Vanderbloemen J *Int. J. Rem. Sen*., 24(13):2597–2612.
[39] Nababan, B 2005. *Bio-optical Variability of Surface Water in the North-eastern Gulf of Mexico*. Ph.D Dissertation. Department of Marine Science, College of Marine Science. University of Florida. 143 pp.
[40] Mannino A, Russ D C and Hooker S B 2008 *Journal of Geophysical Research* 113 (C7): 1–19. doi:10.1029/2007JC004493
[41] Sasaki H, Siswanto E, Nishiuci K, Hasegawa T and Ishisaka J 2008 *Geophysical Research Letter*. 35,L04604,doi:10.1029/2007GL032637.
[42] D'Sa E J and DiMarco S 2009 *Limnology & Oceanography* 54: 2233–2242. DOI:10.4319/ lo.2009.54.6.2233.
[43] Chaichitehrani N. D'Sa E J, Ko D S, Walker N D, Osburn C L and Chen R F 2014 *Journal of Coastal Research* 30 (4): 800–814. DOI:10.2112/JCOASTRESD-13-00036.1.
[44] Yu X, Xiaoa B, Liub X, Wang Y, Cuia B and Liu X 2017 *International Journal of Remote Sensing*, 2017. Vol.38(23):7357–7373 https://doi.org/10.1080/01431161. 2017.1375570.

[45] Wong M S, Lee K H, Kim Y J and Nichol J E 2007 *Korean Journal of Remote Sensing* 23: 161–169.
[46] Khorram S 1982 *Remote Sensing of Environment* 12(1). DOI:10.1016/0034-4257(82) 90004-9
[47] Wang F and Y.J. Xu, 2008. Development and application of a remote sensing-based salinity prediction model for a large estuarine lake in the US Gulf of Mexico coast. *Journal of Hydrology* 360(1-4):184-194 DOI:10.1016/j.jhydrol.2008.07.036
[48] Marghany M and Hashim M 2011 IGARSS 2011, 978-1-4577-1005-6/11/$26.00 ©2011 IEEE pp. 2017-2020
[49] Urquhart E A, Hoffman M J, Murphy R R and Zaitchik B F 2013 Remote Sensing of Environment 135:167-177. DOI: 10.1016/j.rse.2013.03.034
[50] Qing S, Zhang J, Chui T and Bao Y 2013 *Remote Sensing of Environment* 136:117–125, DOI:10.1016/j.rse.2013.04.016
[51] The Editorsof Encyclopaedia Britannica 2017 *Banda Sea* [Internet] accessed Oct 2017 from http://www.britannica.com/place/Banda-Sea
[52] Woythuyzen S, Hukom F D, Makatipu P and Pelasula D 2018 *IOP Conf. Series: Earth and Environmental Science* **184** (2018) 012009 doi :10.1088/1755-1315/184/1/012009
[53] Spooner M I, Barrows T T, De Deckker P and Paterne M 2005 *Global and Planetary Change* 49:28 – 46.
[54] Firdaus M l 2018 *IOP Conf. Series: Earth and Environmental Science* 184 (2018) 012011 doi: 10.1088/ 1755-1315/184/1/012011
[55] Corvianawatie C, Putri M R, Cahyarini S Y and Tatipatta W M. *Indonesia Journal of Geospatial,* https://www.researchgate.net/publication/307136797
[56] Chen, S and Hu, C 2017. *Remote Sensing of Environment 201 (2017) 115–132.* http://dx.doi.org/10/ 1016/j.rse.2017.09.004
[57] Vogel, R L and Christopher W B. 2016. J. Appl. RemoteSens. 10(3), 036003 (2016), doi: 10.1117/1. JRS.10.03600
[58] Marghany M, Hashim M, and Cracknell A P 2010. D. Taniar et al. (Eds.): ICCSA 2010, Part I, LNCS 6016, pp. 545–556, 2010. © Springer-Verlag Berlin Heidelberg 2010
[59] Wouthuyzen S 2002 *Oseanologi dan Limnologi di Indonesia 2002* (34):17-35
[60] Waworuntu J M, Fine R A, Olson D B and Gordon A L 1999. *Submitted to the Journal of Marine Research, July 1999.* 19 pp.
[61] Atmadipoera A S, Prartono T, Jaya I, Nugroho D, Harsono G, Koch-Larrouy A and , Nanlohy P 2019 *IOP Conf. Series: Earth and Environmental Science* **278** (2019) 012008 doi:10.1088/1755-1315/ 278/1/012008
[62] P, Purba N P, Junianto and Sunarto 2018 *World Scientific News 110 (2018) 197-209*